IIETA International Information and Engineering Technology Association
Advancing the World of Information and Engineering

Journal Européen des Systèmes Automatisés
Vol. 58, No. 1, January, 2025, pp. 65-74
Journal homepage: http://iieta.org/journals/jesa

Studying the Effect of Voltage Unbalance on the Working Characteristics of LSPMSM

Anh Tuan Le[1], Nhu Y Do[2], Thac Khanh Nguyen[2*]

[1] Faculty of Electrical Engineering, Hanoi University of Industry, Hanoi 100000, Vietnam
[2] Faculty of Electromechanics, Hanoi University of Mining and Geology, Hanoi 100000, Vietnam

Corresponding Author Email: nguyenthackhanh@humg.edu.vn

https://doi.org/10.18280/jesa.580108

Received: 15 December 2024
Revised: 14 January 2025
Accepted: 21 January 2025
Available online: 31 January 2025

Keywords:
voltage unbalance, permanent magnet, motors, synchronous motors, line start permanent magnet synchronous motors, energy savings

ABSTRACT

With the development of NdFeB rare earth magnet materials, the line-start permanent magnet synchronous motor (LSPMSM) is considered as a alternative method to induction motors for energy savings. During operation, the parameters of LSPMSM are highly susceptible to power quality, particularly the effects of voltage unbalance (VU). This paper focuses on studying the impact of magnitude and phase angle unbalance of the voltage on the operating parameters of a 15 kW, 3000 rpm LSPMSM. The research results indicate that the speed and torque characteristics of the motor are significantly affected by voltage magnitude and phase angle unbalance. However, the current characteristics are largely influenced by voltage magnitude unbalance. Additionally, the power factor cosφ and the efficiency of the motor deteriorate as the degree of unbalance increases. The paper employs Ansys/Maxwell simulation software to study and evaluate the experimental model.

1. INTRODUCTION

Today, with the development of NdFeB rare earth magnet materials, the line-start permanent magnet synchronous motors (LSPMSM) are considered an alternative to the induction motors (IM) for energy savings [1]. The structure of the LSPMSM is similar to that of the IM, with the rotor containing permanent magnet (PM) bars. The LSPMSM is a hybrid between the IM and the interior permanent magnet synchronous motor (IPMSM). Therefore, the LSPMSM has the advantage of synchronous speed, reducing losses due to induced currents in the rotor (which typically account for 20% of total losses), and it has the capability of line-starting. However, the main disadvantage of the LSPMSM is its low starting torque, making it suitable for loads with low starting coefficients, such as fans and electric pumps [2, 3].

During operation, the parameters of the LSPMSM are significantly affected by the power quality of the input power supply. Therefore, there have been numerous studies examining the impact of supply voltage quality on the operation of LSPMSM. The influences of VU on the operational parameters in the steady state of LSPMSM were investigated, including current, losses, and torque ripple. The research findings [4, 5] indicate that when there is VU, the oscillation of the positive sequence current component changes little, while the oscillation of the negative sequence current component is substantial. Additionally, VU also leads to a significant increase in losses in the windings; however, the change in iron core losses is negligible. The study [4] also pointed out that the negative sequence voltage component plays a crucial role in determining the eddy current losses in the rotor, and an increase in VU corresponds to a rise in torque ripple.

The influences of VU and phase unbalance on the working parameters of the motor, including efficiency, power factor, current magnitude, harmonic distortion index, and temperature rise of the LSPMSM and IM are investigated [6, 7]. Based on experimental results, the paper indicates that, compared to equivalent IM, the LSPMSM exhibits more stable efficiency and significantly better power factor under ideal operating conditions. The LSPMSM is less sensitive to variations in voltage magnitude but is highly sensitive to significant levels of VU. According to the study [8], the impact of voltage waveforms containing components with frequencies lower than the fundamental frequency on a 3 kW, 1500 rpm LSPMSM was examined under full load conditions. The research results indicated that the experimental LSPMSM, when supplied with subharmonics of reverse order, exhibited significant oscillations under full load compared to the no-load condition. Thus, the paper suggests that to mitigate the harmful effects caused by subharmonics on users' equipment, regulations should be established to limit them in the quality of the power network.

The impact of voltage drops and cable length on the starting process of the LSPMSM-0.55 kW/3 kW, 1500 rpm used for centrifugal pumps has been demonstrated [9, 10]. The research results indicated that the LSPMSM can start at level of rated voltage, with the voltage reducing to 90% of the rated voltage and through cables under the condition that the voltage drop on the cable does not exceed 4%, as recommended in IEC 60364-5-52 standards. Furthermore, due to the 'soft starting' phenomenon recommended for centrifugal pump applications, motor manufacturers should increase the number of stator winding turns to ensure the starting capability of the

LSPMSM, reduce starting current, and enhance motor efficiency. The impact of harmonics on LSPMSM was investigated in studies [11, 12]. The paper proposes a new calculation method to determine the losses, efficiency, and temperature rise of the motor. The proposed method combines analytical calculations with the finite element analysis (FEA) method. The calculated loss results from the proposed method were compared with experimental results, showing good correlation.

The influences of voltage flicker on the LSPMSM – 4HP under full load conditions was analyzed [13]. The results indicate that under voltage flicker conditions, there is a significant impact on the magnets of the LSPMSM, which in many cases can lead to a complete demagnetization of PM of the motor. The impact of voltage quality on the working conditions of the 0.75 kW, 1800 rpm LSPMSM was demonstrated [14]. Additionally, the effect of voltage on the operating temperature of the motor also is investigated in the paper. The results show that both overvoltage and undervoltage lead to temperatures higher than those at rated voltage, which significantly affects the lifespan of the PMs.

From the analysis above, it is evident that the impact of the quality of the supplied voltage in general, and the phenomenon of VU in particular, on the operating conditions of the LSPMSM is a topic of significant interest. Previous studies have primarily focused on the effect of a single parameter of voltage quality on the operational characteristics of the LSPMSM, without addressing the simultaneous influence of multiple voltage quality parameters on the working conditions of the LSPMSM. Furthermore, prior research has mainly concentrated on LSPMSM operating predominantly at 1500 rpm. This paper focuses on investigating the effects of various voltage quality parameters, including voltage magnitude and phase angle unbalance (VMPAU), on the working characteristics of a 3000 rpm LSPMSM. The results of the study are presented through theoretical analysis, simulations, and assessments using experimental models.

2. MODEL OF THE LSPMSM UNDER VU

2.1 Voltage unbalance

The VU is a situation where the voltage magnitude and phase angle are different [15-17]. According to NEMA, VU is defined as the line voltage unbalance rate (LVUR), which is determined as follows:

$$\%LVUR = \frac{max\ voltage\ deviation\ from\ the\ avg\ LV}{avg\ LV}.100 \quad (1)$$

where, LV-line voltage. According to IEEE standard 112 from 1991, VU is defined as the phase voltage unbalance rate (PVUR), which is determined as follows:

$$\%PVUR = \frac{max\ voltage\ deviation\ from\ the\ avg\ LV}{avg\ phase\ voltage}.100 \quad (2)$$

According to the actual definition: The actual definition of VU is defined as the ratio of the inverse and direct components of the voltage. The percentage VU factor (% VUF), or the actual definition, is determined as follows:

$$\%VUF = \frac{inverse\ voltage\ components}{direct\ voltage\ components}.100 \quad (3)$$

Complex quantities are used when calculating voltage components, such as those related to VU. However, to avoid working with complex numbers, Eq. (4) is used, which approximates Eq. (3).

$$\%voltage\ unbalance = \frac{82.\sqrt{V^2_{abe} + V^2_{bce} + V^2_{cae}}}{avg\ LV} \quad (4)$$

where, V_{abe} is the deviation value between the line voltage V_{ab} and the average line voltage, similarly for V_{bce} and V_{cae}.

2.2 Model of LSPMSM

The general model of the synchronous machine (SM) is presented in Figure 1 [18, 19]:

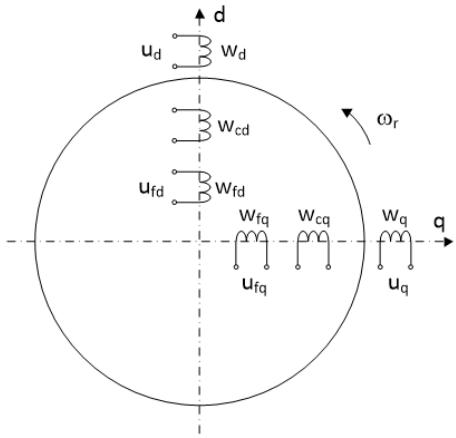

Figure 1. The general model of the SM

where, ω_r- rotor speed, rotor with excitation and damper windings; w_d, w_q - armature winding of the d, q axes; u_d, u_q - winding voltages; w_{cd}, w_{cd} - damper windings of the d, q axes; w_{fd}, w_{fq} - excitation windings of d, q axes; u_f - excitation voltage.

To reduce the number of rotating electromotive force components in the equations, a general diagram is used with the armature winding placed on the rotor (Figure 2).

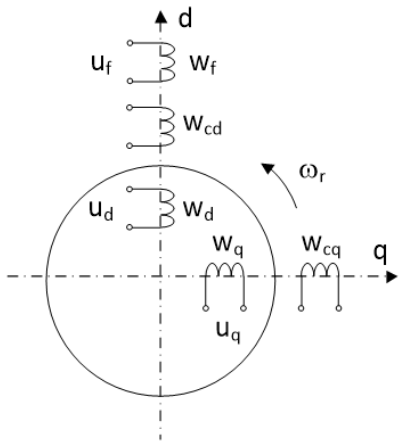

Figure 2. The general model of the SM has the armature winding placed in the stator and the field winding in the rotor

The process of converting electrical to mechanical energy between the windings is independent of whether the windings are stationary or in motion; it only depends on the relative motion of those windings.

The system of equations for the SM is typically described in the d-q coordinate system. If the field is placed in the rotor, the rotor experiences a rotating synchronous magnetic field, inducing an alternating sinusoidal current in the stator winding. Based on the model in Figure 2, the set of voltage balance equations of a synchronous motor is as follows:

$$\begin{cases} u_d = \dfrac{d\Psi_d}{dt} - \Psi_q.\omega_r + r.i_d \\ u_q = \dfrac{d\Psi_q}{dt} + \Psi_d.\omega_r + r.i_q \\ u_f = \dfrac{d\Psi_f}{dt} + r_f.i_f \\ 0 = \dfrac{d\Psi_{cd}}{dt} + r_{cd}.i_{cd} \\ 0 = \dfrac{d\Psi_{cq}}{dt} + r_{cq}.i_{cq} \end{cases} \quad (5)$$

where, i_d, i_q - armature currents of the d, q-axes; i_f – excitation current; i_{cd}, i_{cq} - damper winding currents of the d, q axes.

The flux linkages are defined by the equations:

$$\begin{cases} \Psi_d = L_d.i_d + M_d.i_f + M_d.i_{cd} \\ \Psi_q = L_q.i_q + M_q.i_{cq} \\ \Psi_f = L_f.i_f + M_d.i_d + M_d.i_{cd} \\ \Psi_{cd} = L_{cd}.i_{cd} + M_d.i_d + M_d.i_f \\ \Psi_{cq} = L_{cq}.i_{cq} + M_d.i_q \end{cases} \quad (6)$$

where, L_d, L_q - armature inductances of the d, q axes; L_f - inductance of excitation winding; L_{cd}, L_{cq} - damper inductances of the d, q axes; M_d, M_q - mutual inductances of the d, q axes.

The total inductance is equal to the sum of mutual inductance and leakage inductance ($L = M + L_t$), assuming that the mutual fluxes of the d, q axes are linkage to all windings, while the leakage flux is linkage to only one winding. The torque, T_{el} is defined by the formula (based on the current):

$$T_{el} = M(i_f i_q + i_q i_{cd} - i_d i_{cq}) \quad (7)$$

where, $M = M_d = M_q$ with non-salient pole construction of the rotor.

Or the torque is defined by the formula (based on the magnetic flux linkage).

$$T_{el} = \Psi_d.i_q - \Psi_q.i_d \quad (8)$$

For salient pole electric machines, an additional reactive torque component arises due to the differing magnetic permeability between the d, q axes. The set of equations representing the electromechanical conversion process of the SM is as follows:

$$\begin{cases} u_d = L_d \dfrac{d}{dt} i_d + M_d \dfrac{d}{dt} i_f - L_d i_q \omega_r - M_q i_{cq} \omega_r + r i_d \\ u_q = L_q \dfrac{d}{dt} i_q + M_q \dfrac{d}{dt} i_{cq} + L_d i_d \omega_r + M_d i_f \omega_r + r i_q \\ u_f = L_f \dfrac{d}{dt} i_f + M_d \dfrac{d}{dt} i_d + M_d \dfrac{d}{dt} i_{cd} + r_f i_d \\ 0 = L_{cd} \dfrac{d}{dt} i_{cd} + M_d \dfrac{d}{dt} i_d + M_d \dfrac{d}{dt} i_f + r_{cd} i_{cd} \\ 0 = L_{cq} \dfrac{d}{dt} i_{cq} + M_q \dfrac{d}{dt} i_q + r_{cq} i_{cq} \end{cases} \quad (9)$$

The damper winding only operates when the rotor is oscillating or running at a speed other than synchronous. The damper winding can be neglected, in that case:

$$\begin{cases} u_d = L_d \dfrac{d}{dt} i_d + M_d \dfrac{d}{dt} i_f - L_d i_q \omega_r + r i_d \\ u_q = L_q \dfrac{d}{dt} i_q + L_d i_d \omega_r + M_d i_f \omega_r + r i_q \\ u_f = L_f \dfrac{d}{dt} i_f + M_d \dfrac{d}{dt} i_d + r_f i_d \end{cases} \quad (10)$$

where, $L_d = M_d + L_{td}$, $L_q = M_q + L_{tq}$, $L_f = M_d + L_{tf}$, L_{td}, L_{tq}, L_{tf} - Leakage inductance of the d, q axes and inductance of the excitation winding, substituting the values from (10) into (9) yields:

$$\begin{cases} u_d = L_{td} \dfrac{d}{dt} i_d + M_d \dfrac{d}{dt} i_d + M_d \dfrac{d}{dt} i_f - L_q i_q \omega_r + r i_d \\ u_q = L_q \dfrac{d}{dt} i_q + M_q \dfrac{d}{dt} i_q + L_d i_d \omega_r + M_d i_f \omega_r + r i_q \\ u_f = L_{tf} \dfrac{d}{dt} i_f + M_d \dfrac{d}{dt} (i_f + i_d) + r_f i_f \end{cases} \quad (11)$$

Combining the components with the torque balance equation, the set of equations (voltage balance, torque balance) for the SM is applicable to both steady-state and transient conditions.

$$\begin{cases} E_q = L_q i_q \omega_r E_d = L_d i_d \omega_r + M_d i_d \omega_r \\ u_d = L_{td} \dfrac{d}{dt} i_d + M_d \dfrac{d}{dt} (i_{f+} i_d) - E_q + r i_d \\ u_q = L_{tq} \dfrac{d}{dt} i_q + M_q \dfrac{d}{dt} i_q + E_d + r i_d \\ u_f = L_{tf} \dfrac{d}{dt} i_f + M_d \dfrac{d}{dt} (i_f + i_d) + r_f i_f \\ \sum M = J \dfrac{d\omega_r}{dt} = J \dfrac{d^2\theta}{dt^2} \end{cases} \quad (12)$$

where, J - the moment of inertia; p - the number of pole pairs.

Basically, the LSPMSM model fully inherits the equations of the general synchronous motor model [20]. The mathematical model of the LSPMSM consists of a system of equations for the stator voltage, rotor voltage, stator magnetic flux, and rotor magnetic flux, as given in formulas (13) to (16).

$$\begin{cases} u_{ds} = r_1 i_{ds} + \dfrac{d\Psi_{ds}}{dt} - \omega_r . \Psi_{qs} \\ u_{qs} = r_1 i_{qs} + \dfrac{d\Psi_{qs}}{dt} + \omega_r . \Psi_{ds} \end{cases} \quad (13)$$

$$\begin{cases} u'_{dr} = r'_{dr} i'_{dr} + \dfrac{d\Psi'_{dr}}{dt} = 0 \\ u'_{qr} = r'_{qr} i'_{qr} + \dfrac{d\Psi'_{qr}}{dt} = 0 \end{cases} \quad (14)$$

$$\begin{cases} \Psi_{ds} = (L_{ls} + L_{md}) i_{ds} + L_{md} i'_{dr} + \Psi'_m \\ \Psi_{qs} = (L_{ls} + L_{mq}) i_{qs} + L_{mq} i'_{qr} \end{cases} \quad (15)$$

$$\begin{cases} \Psi'_{dr} = L'_{lr} i'_{dr} + L_{md} (i_{ds} + i'_{dr}) + \Psi'_m \\ \Psi'_{qr} = L'_{lr} i'_{qr} + L_{mq} (i_{qs} + i'_{qr}) \end{cases} \quad (16)$$

where, ω_r - rotor angular velocity; Ψ'_m - stator flux generated by the PMs; L_{ls} - Leakage inductance of the stator winding; L_{md} and L_{mq} - magnetizing inductances of d, q axes; i_{ds}, i_{qs} - stator current of d, q axes; i'_{dr}, i'_{qr} - rotor equivalent current of d, q axes.

The equivalent circuits of LSPMSM in the mathematical model shown in Figure 3 and Figure 4.

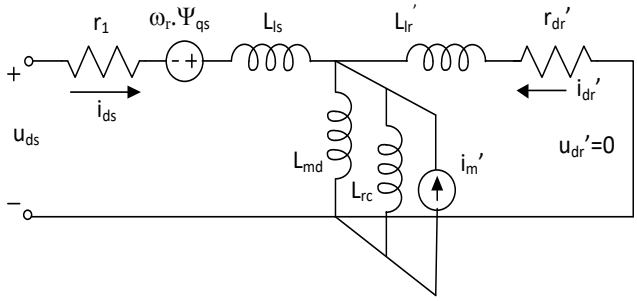

Figure 3. The d-axis equivalent circuit of LSPMSM

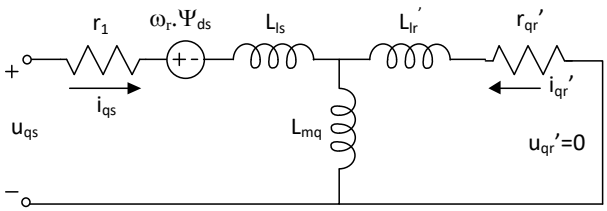

Figure 4. The q-axis equivalent circuit of LSPMSM

The electromagnetic torque of the LSPMSM is determined:

$$M_{el} = \frac{3}{2}.p.\left[\underbrace{\left(L_{md}.i'_{dr}.i_{qs} - L_{mq}.i'_{qr}.i_{ds}\right)}_{Induction\ Torque} + \underbrace{\Psi'_m.i_{qs}}_{Excitation\ Torque} + \underbrace{(L_{md} - L_{mq}).i_{ds}.i_{qs}}_{Reluctance\ Torque}\right] \quad (17)$$

Thus, the electromagnetic torque of the LSPMSM consists of three components: T_{ind} - the induction torque component; T_{exc} - the excitation torque component; T_{rel} - the reluctance torque component. The electromagnetic torque:

$$T_{el} = T_{ind} + T_{exc} + T_{rel} \quad (18)$$

From Eq. (17), it can be observed that the electromagnetic torque of the LSPMSM is much more complex than that of the IM. Thus, the excitation torque and reluctance torque components are equivalent to those of the synchronous reluctance motor. The LSPMSM differs in that it includes an additional induction torque component, which plays a crucial role in the starting capability of the motor [21].

Thus, the model of LSPMSM can be replaced by the IM model and the IPMSM model shown in Figure 5 [22, 23].

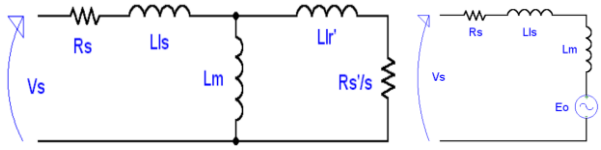

Figure 5. The LSPMSM model includes IM and IPMSM

2.3 VU and LSPMSM torques

In the case of VU, the torque of the IM is significantly affected [24]. At this point, the induction torque component is determined by Eq. (19) below:

$$T_{IM} = \frac{3R_r \left(V_s^1\right)^2 (1\text{-}K_u)}{\left[\left(R_r\right)^2 + (1\text{-}K_u)^2 \left(X_r\right)^2\right].\omega_s} - \frac{3R_r \left(V_s^1\right)^2 (1\text{-}K_u)}{\left[\left(R_r\right)^2 + (1\text{-}K_u)^2 \left(X_r\right)^2\right].\omega_s} \quad (19)$$

where, K_u is the coefficient affected by the VU.

Similarly, the VU also significantly affects the torque of the IPMSM [25].

$$T_{PMSM} = \frac{n_p}{4}.I_m.\psi_f \begin{bmatrix} (3\text{-}k)sin(\omega_e t - \dfrac{n_p}{2}\alpha) \\ +ksin(\omega_e t + \dfrac{n_p}{2}\alpha) \end{bmatrix} \quad (20)$$

The LSPMSM is a combination of the IM and IPMSM, thus the analysis above indicates that the occurrence of VU significantly affects the torque characteristics as well as other working characteristics of the LSPMSM.

3. EFFECT OF VU ON LSPMSM

3.1 Experimental parameters of the LSPMSM

LSPMSM are often used to replace IM to save energy. Due to the small starting torque of LSPMSM, they are typically employed for loads with small starting torque, such as fans and water pumps. In the mining industry, these types of loads often utilize motors with a speed of 3000 rpm and high power, typically in the 15kW range [1]. The effect of VU on the operation of the LSPMSM is investigated in this paper. The paper utilizes a LSPMSM with specifications of 15kW-3,000 rpm in Table 1 [26].

The assessment of the effect of VU on the LPSMSM is conducted using the finite element method (FEM) based on Ansys/Maxwell software. The FEM analysis model of the experimental LSPMSM 15kW, 3000 rpm provided in Table 1 is illustrated in Figure 6.

Table 1. Parameters of LSPMSM

Parameters	Symbol	Value	Unit
Stator outer diameter	D_{in}	245	mm
Stator inner diameter	D_{out}	152	mm
Rotor outer diameter	D'	151	mm
Rotor shaft diameter	D_t	52	mm
Number of stator slots	Z_1	36	slots
Number of rotor slots	Z_2	28	slots
Air gap length	g	0.5	mm
Power supply voltage	U_n	380/660	V
Power supply frequency	f	50	Hz
PM meterial	NdFeBr	SH-38	
Dimension PM rods	$l_m \times w_m \times h_m$	35 × 34 × 9	mm

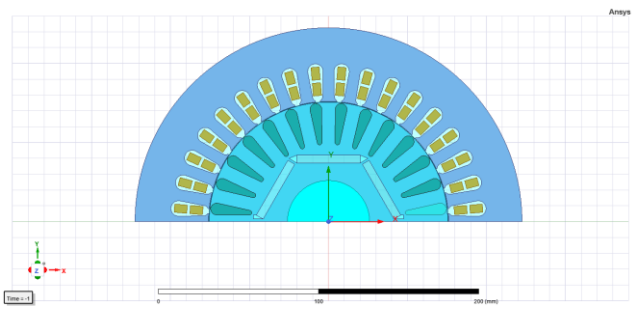

Figure 6. Experimental structure of the rotor of LSPMSM 15kW, 3000 rpm

The impact of VMPAU on the working parameters of the LSPMSM is simulated. Additionally, the paper analyzes the voltage levels increasing/decreasing compared to the rated voltage within a range of ±5%. Additionally, the phase angle deviations of phases b and c vary within a range of 0±12°. The mathematical model of VU is considered as Eq. (20) with five scenarios as shown in Table 2.

$$\begin{cases} U_a = V_{pha}.\sqrt{2}.sin(\omega t) \\ U_b = V_{phb}.\sqrt{2}.sin(\omega t - 120^\circ - \alpha) \\ U_c = V_{phc}.\sqrt{2}.sin(\omega t + 120^\circ - \alpha) \end{cases} \quad (21)$$

Table 2. Simulation scenarios with voltage unbalance

No.	V_a	V_b	V_c
Case 1	380∠0°	380∠-120°	380∠120°
Case 2	380∠0°	370∠-123°	380∠117°
Case 3	380∠0°	370∠-126°	390∠114°
Case 4	360∠0°	370∠-129°	390∠111°
Case 5	370∠0°	390∠-132°	360∠108°

3.2 Simulation and results

3.2.1 Simulation of speed characteristics

The speed characteristics of the motor under phase VU are presented in Figure 7.

Figure 7, it can be seen that in the case of VU, there is a significant impact on the transient characteristics. The unbalance in magnitude, phase angle, or both magnitude and phase angle affect the speed characteristics of the LSPMSM. Main parameters of the speed characteristics are presented in Table 3.

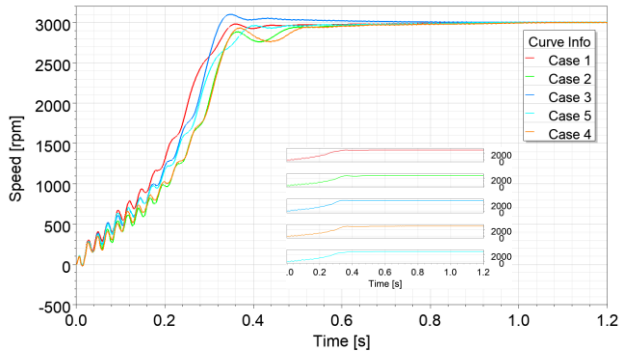

Figure 7. Speed characteristics of LSPMSM

Table 3. Starting characteristics of LSPMSM

No.	t_{st} (s)	t_{tt} (s)	$\Delta\omega_{max}$ (rpm)
Case 1	0.36	0.62	160
Case 2	0.78	0.78	430
Case 3	0.33	0.86	450
Case 4	0.77	0.77	210
Case 5	0.72	0.72	180

Note: t_{st} - synchronization time, t_{tt}-transient time; $\Delta\omega_{max}$ - maximum speed oscillation during the transient time.

Figure 7 and Table 3 indicate that in case 3, the motor synchronizes the fastest (t_{st}=0.33 s). However, the high synchronization speed amplitude causes significant vibrations ($\Delta\omega_{max}$ = 450 rpm) and a long transient time ($t_{tt\ max}$ = 0.86 s). In cases 2 and cases 4, the LSPMSM experiences difficulties during startup and takes a long time to synchronize ($t_{tt\ max}$ = 0.78 s), however the amplitude of the oscillation of the speed decreases ($\Delta\omega_{max}$ = 210 rpm). Besides, in case 5 when the phase angles are varied similarly to case 2 and the phase angle differences are adjusted, it is observed that the starting capability of the LSPMSM improves.

In case 4 and case 5, both have the same magnitude of phase voltage, but the phase shift angle of case 5 (12°) provides better starting characteristics than case 4 (9°). This indicates that along with the amplitude of the voltage, there exists a critical phase shift angle at which the LSPMS exhibits the most difficult starting characteristics. This situation needs to be avoided during the starting process for the LSPMSM.

When there is a phase angle unbalance with a voltage drop in one phase (while the other two phases remain unchanged - case 2), the LSPMSM will have more difficulty starting compared to the case of VU in two phases (one phase's amplitude increases, one phase's amplitude decreases, and one phase's amplitude remains constant - case 4, case 5). Therefore, during operation, it is important to avoid allowing the LSPMSM to operate under conditions of voltage drop, especially a single-phase voltage drop in the power supply.

3.2.2 Torque characteristics of LSPMSM

The simulating results of the torque characteristics of the LSPMSM are presented in Figure 8.

Figure 8, it can be seen that in the case of VU, significant torque oscillations occur. The degree of torque oscillation depends not only on the voltage magnitude and phase angle unbalance but also on both of voltage magnitude and phase

angle. According to the studies [4, 27, 28], the coefficient k is defined to evaluate the torque ripple.

$$k = \frac{T_{\max} - T_{\min}}{T_{\max} + T_{\min}} \quad (22)$$

where, T_{max} and T_{min} are the maximum and minimum values of the instantaneous torque, respectively. During the starting period (Figure 8), the maximum torque ripple coefficient is observed, $k_{max\_starting}$ = 9.2 corresponding to case 5. Compared to the balanced voltage (case 1-where $k_{max\_starting}$ = 4.1), the maximum torque ripple coefficient in case 5 increases by a factor of 2.24.

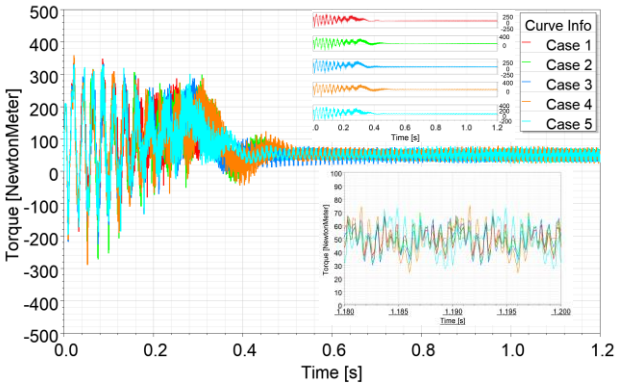

Figure 8. Torque characteristics of the experimental LSPMSM

In the steady-state time, the maximum torque ripple coefficient is $k_{max\_steadystate}$ = 0.51 for case 5. Compared to the balanced voltage, the maximum torque ripple coefficient in case 5 increases by a factor of 1.55.

Synthesis of the maximum torque ripple coefficient evaluation in the two modes of transient and steady state period, as shown in Table 4.

Table 4. Torque ripple coefficient at transient and steady state period

No.	Transient Time of Torque (s)	Transient Period Torque Ripple Coefficient, k_{max}	Steady State Period Torque Ripple Coefficient, k_{max}
Case 1	0.49	4.1	0.33
Case 2	0.54	5.6	0.35
Case 3	0.59	6.2	0.38
Case 4	0.61	8.5	0.47
Case 5	0.65	9.2	0.51

Table 4 indicate that the transient time of torque increases when there is a phase angle unbalance. As the phase angle unbalance increases, the torque ripple coefficient k also increases. At the steady state, k_{max} reaches k = 0.51 when the phase shift angle α=12° compared to k = 0.33 when there is no phase shift. This explains that the motor operates with more vibration and acoustic noise when phase angle unbalance occurs.

3.2.3 Current characteristics

Due to the VU, the current characteristics of each phase will differ. The current characteristics of phase A are simulated under scenarios of VU as shown in Figure 9, and the fast fourier transform (FFT) analysis of the harmonic orders of phase A current is presented in Figure 10.

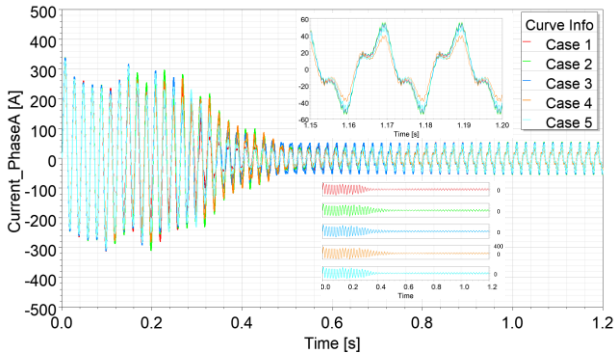

Figure 9. Current characteristics of phase A in steady-state time

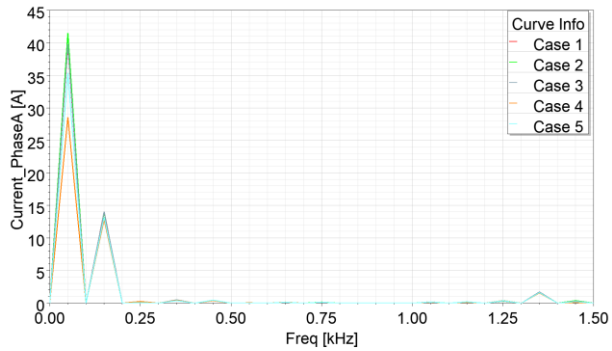

Figure 10. FFT analysis of the harmonic orders of phase A current

The level of current harmonic generation of LSPMSM is evaluated, the total harmonic distortion index (THD_i) is used, which is determined according to the formula [29, 30]:

$$THD_i = \frac{\sqrt{\sum_{n=2}^{\infty} I_n^2}}{I_1} \quad (23)$$

The results of the THD_i analysis in cases of VMPAU in Table 5.

Table 5. Simulation scenarios with voltage unbalance

No.	THDi		
	Phase A	Phase B	Phase C
Case 1	35.91%	35.9%	35.89%
Case 2	34.04%	40.1%	34.08%
Case 3	35.74%	42.7%	31.10%
Case 4	45.41%	38.0%	28.35%
Case 5	37.73%	28.2%	45.12%

From Figure 9, Figure 10 and Table 5, it can be seen that in case 1, considering phase unbalance, the THD_i of the working current of the LSPMSM is relatively high (35.9%). In case 2, the THD_i of phases A and C decreases slightly, while the THD_i of phase B (40.1%) increases significantly compared to case 1. In case 3, the THD_i of current phase A remains almost unchanged, with current phase B showing a slight increase (41.7%), while current phase C decreases significantly (31.1%) compared to case 1. In case 4, the THD_i of current phase A increases considerably (45.41%), the THD_i of current phase B increases slightly (38%), and the THD_i of current phase C

decreases (28.35%). In case 5, the THD_i of current phase A increases slightly (37.73%), the THD_i of current phase B decreases (28.2%), while the THD_i of current phase C significantly increases (45.12%).

It can be seen that a phase angle deviation ranging from 0 to 12° has little impact on the THD_i of the current. However, a voltage magnitude unbalance of about 5% significantly affects the THD_i of the current.

3.2.4 Efficiency and power factor of LSPMSM

Simulating results of the efficiency and power factor characteristics of the LSPMSM under VU are presented in Figure 11 and Figure 12.

In Figure 11 and Figure 12, the efficiency and power factor cosφ in the steady-state time of the LSPMSM are presented in Table 6.

From the results in Table 6, it can be observed that due to the influence of higher-order harmonics, the efficiency and power factor cosφ of the motor gradually decrease. This result is consistent with the analysis that the harmful effects of current harmonics lead to losses that reduce the operational efficiency of the motor.

Table 6. Simulation scenarios with voltage unbalance

Type	η	Cosφ
Case 1	0.9382	0.9468
Case 2	0.9264	0.8831
Case 3	0.9182	0.8571
Case 4	0.8997	0.8294
Case 5	0.8879	0.7892

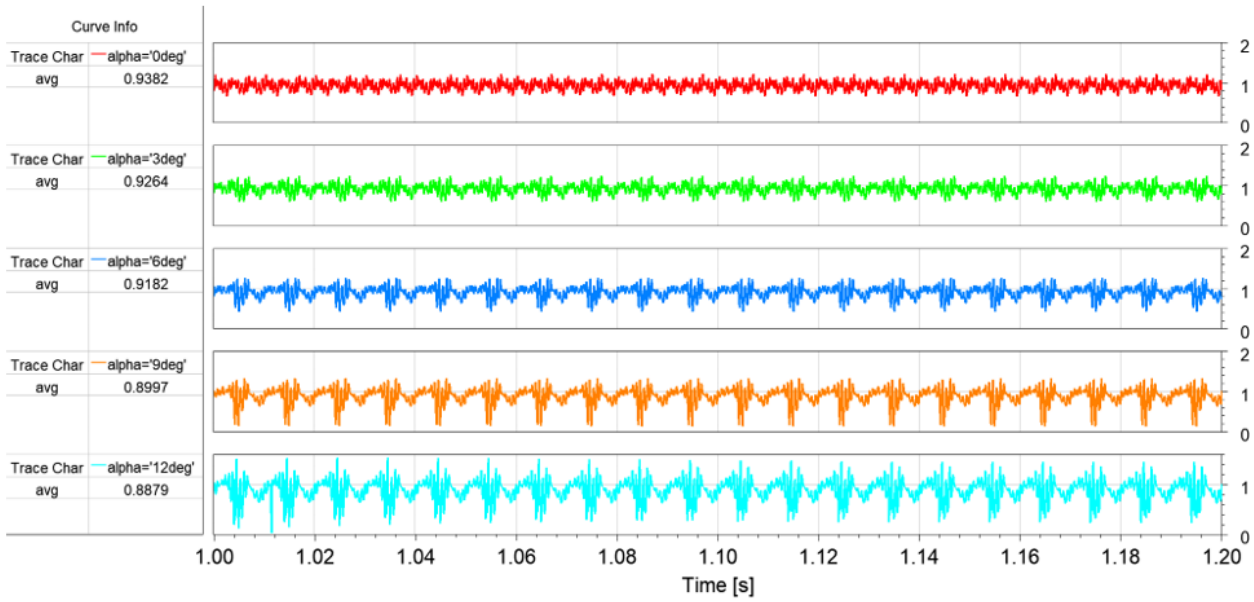

Figure 11. Efficiency characteristics

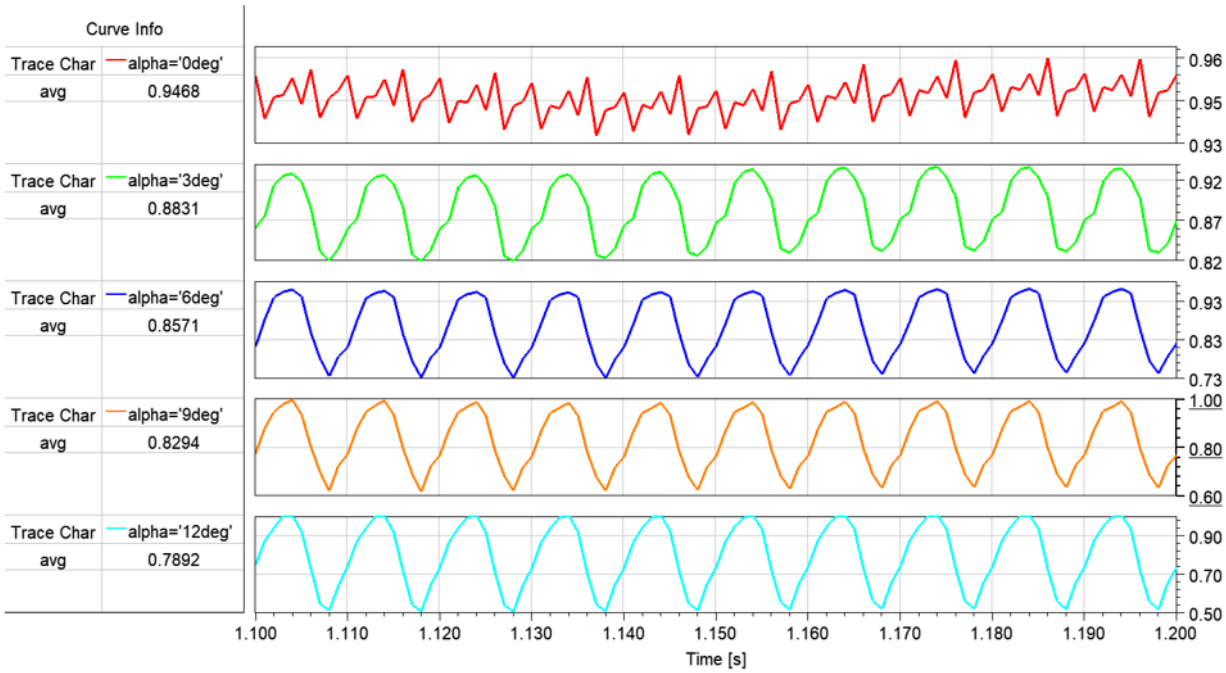

Figure 12. Power factor characteristics, cosφ

4. EXPERIMENTATION

The experimental evaluation was conducted in the laboratory of the Faculty of Electromechanics at Hanoi University of Mining and Geology. The experimental principal diagram is shown in Figure 13.

The testing process was conducted by varying the single-phase loads (load A, load B, load C), resulting in VMPAU in the voltage supplied to the LSPMSM corresponding to case 4. The testing results are measured using the KYORITSU 6310 multifunction power analyzer, which recorded several signals related to voltage, current, and power factor cosφ. The current characteristics of phase A measured by the KYORITSU 6310 during the testing process are presented in Figure 14.

The current characteristics in Figure 14 indicate that when phase VU occurs, the current of the LSPMSM is no longer sinusoidal like that of the IM. However, the LSPMSM exhibits a significant level of non-sinusoidal behavior. In addition to the non-sinusoidal level, the current characteristics of the LSPMSM show a peaked shape at the beginning of the half-cycle, indicating that the motor's magnetic circuit has saturated. The current characteristics at the end of the half-cycle exhibit a sharp peak, causing a surge in current. At this point, this can lead to demagnetization of the PM, potentially causing the LSPMSM to malfunction and resulting in motor damage.

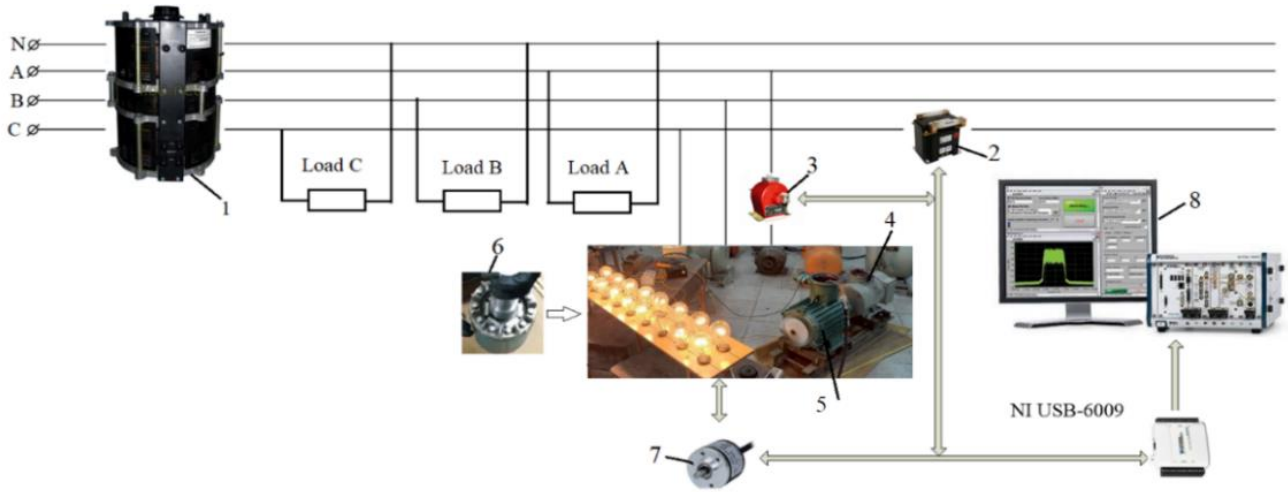

Figure 13. Experimental principle diagram of LSPMSM
Note: 1 - Auto transformer; 2 - Voltage transformer; 3 - Current transformer; 4 - Testing load;
5 - Experimental LSPMSM;6-Rotor of LSPMSM; 7 - Encoder; 8- Displaying device

Figure 14. Measured current characteristic of phase A of LSPMSM

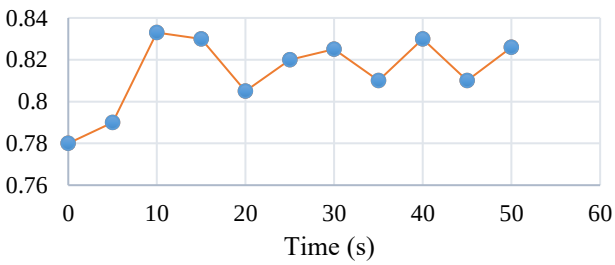

Figure 15. Cosφ characteristics of LSPMSM in testing

Figure 14 also indicates that the current characteristics during the testing process closely similar to the current waveform simulated in Figure 9, additionally the measured current has a high THD_i when analyzing FFT of the current harmonic of phase A, in this case THD_i = 48.8%. This measured value is close to the THD_i value obtained from the simulation evaluation in Table 4 (THD_i = 45.41%). Similarly, the investigation of the power factor cosφ of the LSPMSM obtained during the testing process is presented in Figure 15.

Figure 15 indicates that the cosφ varies and fluctuates significantly during VU time. In the steady-state time, the cosφ is equal to 0.826, which is similar to the cosφ obtained during the simulation (0.8294). Thus, it can be observed that with the limited experimental model, the investigation of the current signals and cosφ shows that the experimental results are somewhat consistent with the theoretical and experimental values obtained.

5. CONCLUSIONS

The LSPMSM is designed to operate under sinusoidal of voltage supply, three-phase conditions with voltage magnitude and phase angle. However, in practice, the voltage supplied to the LSPMSM is often unbalanced, affecting the motor's performance characteristics. Evaluating the impact of VU on working characteristics will enhance the operational quality of the LSPMSM in reality. This paper focuses on studying the influences of VMPAU on the working characteristics of a 15kW-3000rpm LSPMSM. The paper utilizes Ansys/Maxwell software to simulate the motor's characteristics, and some results were also tested on a experimental LSPMSM. The research results indicate that the speed and torque characteristics of the LSPMSM are significantly affected by

VMPAU. However, the current characteristics are greatly influenced by voltage magnitude unbalance, and additionally, the power factor cosφ and efficiency of the motor deteriorate as the level of VU increases.

Through analysis, it is observed that in the case of phase VU, there exists a critical phase shift angle at which the starting process becomes the most difficult. Additionally, when there is phase angle unbalance and a voltage drop occurs in one phase while the voltage magnitudes of the other two phases remain constant, the LSPMSM will start more difficultly compared to when there is unbalance between two phases (where one phase has an increased magnitude, one phase has a decreased magnitude, and one phase remains constant). Furthermore, when there is phase angle unbalance, the current of the LSPMSM exhibits a strong level of non-sinusoidal behavior. The current characteristics of the LSPMSM show a peaked shape at the beginning of the half-cycle, indicating that the motor's magnetic circuit is saturated. The current characteristics at the end of the half-cycle exhibit a sharp peak, causing a surge in current. At this point, this can lead to demagnetization of the PMs resulting in the LSPMSM malfunctioning and causing motor damage.

Additionally, the phenomenon of VU also increases the torque ripple of the motor compared to normal conditions. During the transient period, the torque coefficient reaches $k_{\text{max\_starting}} = 9.2$, and during steady-state operation, $k_{max\_steadystate} = 0.51$. Furthermore, the efficiency and power factor of the LSPMSM are significantly reduced, sometimes falling below the parameters of the IM. Therefore, to ensure the LSPMSM operates effectively, it is essential to implement solutions to improve the quality of the power supply provided to the motor.

REFERENCES

[1] Do Nhu, Y., Thuy, T.B., Cuong, N.X. (2024). Rotor configuration for improved working characteristics of LSPMSM in mining applications. Natsional'nyi Hirnychyi Universytet. Naukovyi Visnyk, 3: 79-86. https://doi.org/10.33271/nvngu/2024-3/079

[2] De Souza, E. (2015). Improving the energy efficiency of mine fan assemblages. Applied Thermal Engineering, 90: 1092-1097. https://doi.org/10.1016/j.applthermaleng.2015.04.048

[3] Biyani, V., Jinesh, R., TA, T.E., VS, S.S. (2022). Vector control implementation in PMSM motor drive for electric-vehicle application. In 2022 4th International Conference on Energy, Power and Environment (ICEPE), Shillong, India, pp. 1-8. https://doi.org/10.1109/ICEPE55035.2022.9798140

[4] Qiu, H., Hu, K., Yi, R., Wei, Y. (2019). Influence of voltage unbalance on the steady-state performance of line start permanent magnet synchronous motors. IEEJ Transactions on Electrical and Electronic Engineering, 14(11): 1673-1680. https://doi.org/10.1002/tee.22990

[5] Sethupathi, P., Senthilnathan, N. (2020). Comparative analysis of line-start permanent magnet synchronous motor and squirrel cage induction motor under customary power quality indices. Electrical Engineering, 102(3): 1339-1349. https://doi.org/10.1007/s00202-020-00955-2

[6] Ferreira, F.J.T.E., De Almeida, A., Cistelecan, M. (2009). Voltage unbalance impact on the performance of line-start permanent-magnet synchronous motors. In Proceedings of the 6th International Conference EEMODS, Nantes, France, pp. 14-17.

[7] Orság, P., Kocman, S., Otýpka, J. (2014). Impact of mains power quality on operation characteristics of induction motor. In 2014 14th International Conference on Environment and Electrical Engineering, Krakow, Poland, pp. 382-385. https://doi.org/10.1109/EEEIC.2014.6835898

[8] Gnaciński, P., Pepliński, M., Muc, A., Hallmann, D. (2023). Line-start permanent magnet synchronous motor supplied with voltage containing negative-sequence subharmonics. Energies, 17(1): 91. https://doi.org/10.3390/en17010091

[9] Paramonov, A., Oshurbekov, S., Kazakbaev, V., Prakht, V., Dmitrievskii, V. (2023). Investigation of the effect of the voltage drop and cable length on the success of starting the line-start permanent magnet motor in the drive of a centrifugal pump unit. Mathematics, 11(3): 646. https://doi.org/10.3390/math11030646

[10] Tabora, J.M., de Matos, E.O., Soares, T.M., Tostes, M.E.D.L. (2020). Voltage unbalance effect on the behavior of IE2, IE3 and IE4 induction motor classes. Simpósio Brasileiro de Sistemas Elétricos-SBSE, 1(1): 2345. https://doi.org/10.48011/sbse.v1i1.2345

[11] Sethupathi, P., Senthilnathan, N., Ravisankar, B., Lenin, N.C. (2022). Voltage harmonics impact on line start permanent magnet synchronous motor: A new computational method. Arabian Journal for Science and Engineering, 47(11): 14377-14388. https://doi.org/10.1007/s13369-022-06764-y

[12] Thuy, T.B., Cuong, N.X., Tuan, L.A., Do Nhu, Y. (2023). Effect of permanent magnet structure on working characteristics of LSPMSM 3000 rpm. In IOP Conference Series: Earth and Environmental Science, Jakarta, Indonesia, p. 012049. https://doi.org/10.1088/1755-1315/1275/1/012049

[13] Ugale, R.T., BalaKrishna, Y., Chaudhari, B.N. (2008). Effects of short power interruptions and voltage sags on the performance of line start permanent magnet synchronous motor. In IET 4th International Conference on Power Electronics, Machines & Drives, United Kingdom, pp. 184-188. https://doi.org/10.1049/cp:20080508

[14] Tabora, J.M., Correa dos Santos Júnior, L., Ortiz de Matos, E., Mota Soares, T., Arrifano Manito, A.R., de Lima Tostes, M.E., Holanda Bezerra, U. (2023). Exploring the effects of voltage variation and load on the electrical and thermal performance of permanent-magnet synchronous motors. Energies, 17(1): 8. https://doi.org/10.3390/en17010008

[15] Knezevic, B.Z. (2023). Analysis of voltage asymmetry in mechatronic systems: Modeling and experimental validation. Proceedings of VIAC in October 2023, p. 74.

[16] Do Nhu, Y., Cuong, N.X. (2022). Impact of voltage unbalance and harmonics on induction motor in operation mode. In Advances in Engineering Research and Application: Proceedings of the International Conference on Engineering Research and Applications, ICERA 2021, Springer Cham, pp. 468-478. https://doi.org/10.1007/978-3-030-92574-1_49

[17] Adekitan, A.I. (2020). A new definition of voltage unbalance using supply phase shift. Journal of Control,

Automation and Electrical Systems, 31(3): 718-725. https://doi.org/10.1007/s40313-020-00579-8
[18] Cardenas, J. (2022). Book on Electric Machines. Basic Theory.
[19] Sanusi. K.A., Olatomiwa, L., Mohammed, A.D., Sodiq, K.A. (2022) Capacitively-excited single-phase asynchronous generator for autonomous applications. Nigerian Journal of Technological Development, 19(2): 128-135. https://doi.org/10.4314/njtd.v19i2.4
[20] Soreshjani, M.H., Sadoughi, A. (2014). Conceptual comparison of line-start permanent magnet synchronous and induction machines for line-fed of different conditions. Journal of World's Electrical Engineering and Technology, 3(1): 26-36.
[21] Soreshjani, M.H., Heidari, R., Ghafari, A. (2014). The application of classical Direct Torque and Flux Control (DTFC) for line-start permanent magnet synchronous and its comparison with permanent magnet synchronous motor. Journal of Electrical Engineering and Technology, 9(6): 1954-1959. https://doi.org/10.5370/JEET.2014.9.6.1954
[22] Taylor, N. (2001). Network effects of line start permanent magnet synchronous motors as replacements for induction motors. Department of Electrical Power Engineering, Royal Institute of Technology, Stockholm.
[23] Shestakov, A.V., Zhelnin, V.V., Ismiev, R.N. (2016). An experimental study of the operating characteristics of an asynchronous motor with pulse supply. Russian Electrical Engineering, 87: 333-339. https://doi.org/10.3103/S1068371216060080
[24] Do, Y.N., Le, T.X., Nguyen, N.B., Ngo, T.T. (2020). Impact of asymmetrical phenomena on asynchronous three-phase motors in operation mode. Journal of Mining and Earth Sciences, 61(3): 68-74. https://doi.org/10.46326/JMES.2020.61(3).08
[25] Zhao, X.D., Corda, J., Mei, T.X. (2010). Analysis of the effect of asymmetrical phase parameters in a 3-phase permanent magnet synchronous motor. In the XIX International Conference on Electrical Machines-ICEM 2010, Rome, Italy, pp. 1-6. https://doi.org/10.1109/ICELMACH.2010.5608237
[26] Thuy, T.B., Tuan, L.A., Nhu Y.D., Cuong, N.X. (2023). Influence of the NdFeB permanent magnet on working characteristics of LSPMSM. In International Conference on Engineering Research and Applications, Springer Cham, pp. 61-67. https://doi.org/10.1088/1755-1315/1275/1/012049
[27] Do, N.Y., Ngo, X.C. (2022). Effect of voltage unbalance on matrix converter induction motor drive. In Advances in Engineering Research and Application, Springer Cham, pp. 468-476. https://doi.org/10.1007/978-3-031-22200-9_53
[28] Do, N.Y., Ngo, X.C. (2021). Influence of single-phase voltage loss and load carrying mode on mine drainage pump motor in Vietnam. Inżynieria Mineralna. https://doi.org/10.29227/IM-2021-02-31
[29] Do, N.Y., Ngo, X.C. (2022). Effect of harmonic components and load carrying factor on the operating mode of induction motor. In 2nd International Symposium of Earth, Energy, Environmental Science and Sustainable Development 2021, Jakarta, Indonesia, p. 020004. https://doi.org/10.1063/5.0105148
[30] Grajales, J., Ramírez, J., Cadavid, D. (2004). Effects of harmonics in the induction motors: A review. Revista Facultad de Ingeniería Universidad de Antioquia, 31: 116-123. https://doi.org/10.17533/udea.redin.344514